Projection-Resolved Optical Coherence Tomographic Angiography of Retinal Plexuses in Retinitis Pigmentosa

AHMED M. HAGAG, JIE WANG, KEVIN LU, GARETH HARMAN, RICHARD G. WELEBER, DAVID HUANG, PAUL YANG, MARK E. PENNESI, AND YALI JIA

• PURPOSE: To use projection-resolved optical coherence tomographic angiography (PR-OCTA) to characterize the microvascular changes in 3 distinct retinal plexuses in retinitis pigmentosa (RP) patients.
• DESIGN: Prospective cross-sectional study.
• METHODS: A commercial 70-kHz spectral-domain optical coherence tomography (OCT) system was used to acquire 6-mm macular scans from RP patients and age-matched healthy participants at a tertiary academic center. Blood flow was detected using a commercial version of split-spectrum amplitude-decorrelation angiography (SSADA) algorithm. The PR-OCTA algorithm was used to suppress projection artifacts and resolve microvasculature in 3 plexuses around the macula. Vessel density was calculated from *en face* OCTA of the parafoveal and perifoveal regions in each of the 3 plexuses, as well as the all-plexus inner retinal slab. Inner and outer retinal thicknesses were measured form structural OCT scans. Generalized estimating equations and Spearman's rank correlation statistical methods were used.
• RESULTS: Forty-four eyes from 26 RP patients and 34 eyes from 26 healthy subjects were included. Significant reduction in vessel density was detected in the perifovea but not the parafovea of inner retinal slab of RP patients ($P = .001$ and $P = .56$, respectively) compared to controls. We also found deeper retinal plexuses (intermediate and deep capillary plexuses, ICP and DCP) were primarily damaged by RP, compared to superficial vascular complex (SVC). Significant thickening of the inner retina and thinning of the outer retina were also observed. Strong correlation was found between the vessel density in the perifoveal ICP and DCP and outer retinal thickness in RP patients with no history of cystoid macular edema.
• CONCLUSIONS: PR-OCTA enables the detection of microvascular changes in the perifoveal regions of the ICP and DCP in RP, with relative sparing of the SVC. OCT and OCTA parameters might be able to provide better understanding of the pathophysiology of the disease, as well as monitoring disease progression and the response to experimental treatments. (Am J Ophthalmol 2019;204:70–79. © 2019 Elsevier Inc. All rights reserved.)

RETINITIS PIGMENTOSA (RP) IS A GROUP OF HEREDITARY retinal diseases characterized by progressive degeneration of rod and cone photoreceptors. To date, RP has been associated with mutations in at least 64 genes,[1] and inheritance can follow autosomal recessive, autosomal dominant, or X-linked recessive patterns.[1,2] Affected individuals typically experience nyctalopia in adolescence, followed by loss of peripheral vision, and eventually loss of central vision.[1] RP is a leading cause of blindness in individuals under 60 years of age.[3] Global prevalence is about 1 in 4000, with a total of over 1 million affected individuals worldwide.[2,4]

A wide array of therapeutic approaches to RP have been considered.[5,6] However, in order for these treatments to be successfully tested in clinical trials, consistent and well-defined measurements of disease progression are needed to evaluate therapeutic outcomes. Currently, clinical assessment consists of measures that include visual acuity, visual fields, cone and rod electroretinograms (ERG), and optical coherence tomography (OCT).[1] Since good visual acuity can persist for many years even in patients with severe retinal degeneration, clinical studies typically employ ERG amplitudes and visual field sensitivity to assess disease severity, progression, and response to treatment.[7–9] However, ERG and visual fields can demonstrate relatively high test-retest variability.[10,11] ERGs are often extinguished in many patients with RP, and visual field measurements are subjective and dependent on patient cooperation. In contrast, OCT[12] can provide reliable and objective structural information of the retina that has been found to correlate with retinal function.[13–15]

Fluorescein angiography (FA) has previously been used for qualitative evaluation of vascular changes in RP.[16]

AJO.com Supplemental Material available at AJO.com.
Accepted for publication Feb 22, 2019.

From the Casey Eye Institute, Oregon Health & Science University, Portland, Oregon, USA (A.M.H., J.W., K.L., G.H., R.G.W., D.H., P.Y., M.E.P., Y.J.); Moorfields Eye Hospital NHS Foundation Trust, London, United Kingdom (A.M.H.); Institute of Ophthalmology, University College London, London, United Kingdom (A.M.H.); Department of Biomedical Engineering, Oregon Health & Science University, Portland, Oregon, USA (J.W., Y.J.); and Donald and Barbara Zucker School of Medicine at Hofstra/Northwell, Hempstead, New York, USA (K.L.).

Inquiries to Yali Jia, Casey Eye Institute, Oregon Health and Science University, 3375 SW Terwilliger Boulevard, Portland, OR 97239; e-mail: jiaya@ohsu.edu

0002-9394/$36.00
https://doi.org/10.1016/j.ajo.2019.02.034

Attenuation of retinal and choroidal vasculature is typical in patients with RP.[2,17,18] However, FA is invasive, exposes the patient to potentially damaging light, and is not depth-resolved. This results in a time-consuming process that does not distinguish between different layers of retinal circulation.[19,20] More recently, OCT angiography (OCTA),[21] a functional extension of OCT technology, has been proposed as a noninvasive modality for 3-dimensional visualization and quantification of retinal macrovasculature and microvasculature.[22–24] Characterizing the changes in retinal hemodynamics using OCTA might help better understand the pathophysiology of RP.[25] Furthermore, quantifying vascular changes might provide an objective and reliable substitute for monitoring RP progression and response to treatment, since correlation was previously reported between retinal perfusion and visual function.[26,27]

Conventional OCTA images suffer from projection artifacts, in which flow signal from superficial blood vessels is projected onto deeper vascular plexuses.[22,24,28] This limits the ability to accurately separate and quantify OCT angiograms into the 3 distinct macular vascular layers described in histologic studies: superficial vascular complex (SVC), intermediate capillary plexus (ICP), and deep capillary plexus (DCP).[29] Thus, previous investigations of OCTA in RP described microvascular changes in up to 2 vascular layers: the superficial and deep capillary plexuses,[30–32] dividing the ICP between the superficial and deep layers. Two-layer segmentation could lead to inaccurate quantification of retinal perfusion.

Our group has recently developed a projection-resolved OCTA (PR-OCTA) algorithm[33,34] to significantly suppress projection artifacts, allowing for proper segmentation of retinal circulation, and in turn more reliable visualization and quantification of microvasculature.[35–45] In this study, we aim to characterize the alterations in perfusion in all 3 retinal plexuses, as well as the relationship between vascular and structural changes in RP patients.

METHODS

• **STUDY POPULATION:** Patients and age-matched healthy volunteers were recruited from the Ophthalmic Genetics clinic at the Casey Eye Institute at Oregon Health & Science University. An informed written consent was obtained from all participants. This prospective cross-sectional study was approved by the institutional review board of Oregon Health & Science University and all study procedures were done in accordance with the tenets of the Declaration of Helsinki. All participants underwent comprehensive ophthalmologic examination. RP patients were diagnosed by an inherited retinal degeneration specialist based on history, fundus appearance, OCT structure, kinetic and static perimetry, and electroretinograms. Patients were graded by an experienced ophthalmologist into 3 severity groups based on the horizontal width of central visual field to the V4e target. The mild group included patients with more than 110 degrees, moderate groups was between 30 and 110 degrees, and the severe group included patients with less than 30 degrees of central visual field. Patients were excluded if they had any of the following: (1) retinal disease other than RP; (2) systemic disease that has a known effect on retinal vasculature, such as diabetes or hypertension; (3) an ophthalmic condition that would interfere with OCT data acquisition, such as severe nystagmus or media opacity; or (4) history of ocular trauma or major surgery other than uncomplicated cataract surgery. Exclusion criteria for control subjects included ocular disease, inability to maintain fixation for scanning, visual acuity worse than 20/40, significant media opacity, or history of major ocular surgery.

• **OPTICAL COHERENCE TOMOGRAPHY AND OPTICAL COHERENCE TOMOGRAPHY ANGIOGRAPHY:** All study participants underwent OCT scanning using a commercially available spectral-domain OCT system (RTVue-XR; Optovue, Inc., Fremont, California, USA). The system has a repetition frequency of 70k A-scans per second. The device works at a center wavelength of 840 nm and a bandwidth of 45 nm, with axial and transverse resolutions of 5 μm and 22 μm in tissue, respectively. Macular 6×6-mm^2 scans were acquired. Each data set consisted of 2 registered volumetric scans with orthogonal directions (X-fast and Y-fast). Each volumetric scan consisted of 304 A-scans in the fast scanning direction at 304 locations in the slow scanning direction. Two B-scans were acquired at each location and the angiography data were obtained using a built-in commercial version of the split-spectrum amplitude-decorrelation angiography algorithm.[21] Thus, both structural and angiographic data were obtained simultaneously.

• **DATA PROCESSING:** An expert grader reviewed the acquired OCTA images for quality control. Scans with low signal strength index (<50), significant motion artifacts, or defocusing, as well as off-center scans, were excluded. The included structural OCT scans were segmented using a directional graph search method[46] (Figure 1). The retina was segmented at the inner limiting membrane (ILM), inner plexiform layer (IPL), inner nuclear layer (INL), outer plexiform layer (OPL), and Bruch membrane (BM).

Our novel reflectance-based projection-resolved OCTA algorithm[34] was used to suppress projection artifacts and visualize OCT angiograms of 3 distinct retinal vascular layers in the macula. En face angiograms were constructed by maximum projection of flow signal at specific slabs (Figure 1). The inner retinal slab was defined between the ILM and the outer boundary of the OPL. The inner retina was then subdivided into 3 vascular layers: SVC, ICP, and DCP. The SVC lies in the inner 80% of the ganglion cell complex (GCC: layers between ILM and outer

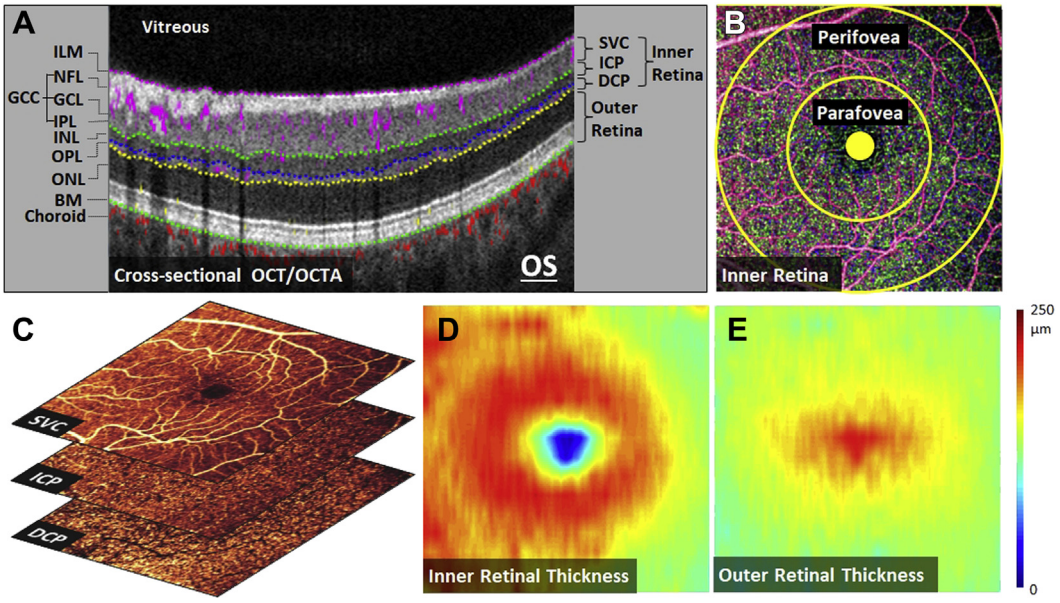

FIGURE 1. Optical coherence tomography (OCT) and OCT angiography (OCTA) data (6 × 6 mm^2 scans) from the left eye of a healthy participant representing the processing methods. (A) Cross-sectional OCTA with color-coded flow signal overlaid on gray-scale reflectance signal. The segmented retinal layers are internal limiting membrane (ILM), nerve fiber layer (NFL), ganglion cell layer (GCL), ganglion cell complex (GCC), inner plexiform layer (IPL), inner nuclear layer (INL), outer plexiform layer (OPL), outer nuclear layer (ONL), and Bruch membrane (BM). (B) Inner retinal OCT angiogram consisting of color-coded retinal plexuses; superficial vascular complex (SVC, violet), intermediate capillary plexus (ICP, green), and deep capillary plexus (DCP, blue). The yellow circles show the boundaries of perifoveal and parafoveal regions. The foveal avascular zone (solid circle, 0.6 mm diameter) was excluded from vessel density analysis. (C) OCT angiograms of the SVC, ICP, and DCP. (D, E): Color-coded inner and outer retinal thickness maps, respectively.

boundary of IPL). The ICP was located in the outer 20% of the GCC and inner 50% of the INL layer. The DCP was detected in the outer 50% of the INL and all of the OPL.

The en face OCT images were divided into parafoveal and perifoveal regions outside the manually centered 0.6-mm-diameter foveal avascular zone (FAZ) (Figure 1). The parafoveal region was defined as an annulus region between the FAZ and an external circle of 3 mm diameter. The perifoveal region lies outside the parafoveal region, and extends to an external circle of 6 mm diameter.

Vessel density (VD) was measured from the en face OCT angiograms as the percent area of pixels occupied by vascular flow signal.[22] The average reflectance in the INL, OPL, and ONL is used to adjust the threshold flow signal value to classify vessel vs static tissue on en face OCTA.[47] VD was calculated in the parafoveal and perifoveal regions (Figure 1). Even with projection resolution, large vessels in the SVC can still produce shadowing artifacts on the deeper layers. Therefore, areas of large vessel were identified from the inner retinal slab[48] and excluded from VD calculation in the ICP and DCP.

Outer and inner retinal thickness were measured to assess the structural changes. Outer retinal thickness was calculated between the outer boundary of the OPL and BM. Meanwhile, inner retinal thickness was measured from the ILM to the outer boundary of the OPL. Care was taken during image acquisition to ensure scans were not tilted to avoid the variation in the intensity of the Henle layer. The distances between layers' boundaries were measured at each A-scan to generate color thickness maps of the outer and inner retinal slabs (Figure 1).

• **STATISTICAL ANALYSIS:** Statistical analysis was performed using Microsoft Excel 2013 (Microsoft Office, Microsoft Corporation, Redmond, Washington, USA) and SPSS v. 24.0 (IBM Corporation, Armonk, New York, USA). Vessel density and thickness measurements are presented as mean and standard deviation (SD) of the included subjects in each group. Analysis of variance (-ANOVA) test was used to assess if there is significant difference in age and visual acuity between groups. If statistically significant difference was found using ANOVA, Games-Howell nonparametric post hoc test would be used to confirm where the differences occurred between groups. Generalized estimating equations were used to compare the vascular, structural, and functional measurements between the groups, accounting for the within-subject correlations arising from using both eyes from the same subjects. Significant P values were adjusted for multiple comparisons using the Holm-Bonferroni method. Likelihood ratio χ^2 test was used to assess the

TABLE 1. Characteristics of Participants and Eyes Included

		RP	
	Control	No CME	CME
Participants	26	13	13
Sex			
Male	15	3	9
Female	11	10	4
Genetic testing	NA	11	11
Mutation found	NA	7	7
Inconclusive	NA	2	4
Mode of inheritance			
Autosomal dominant	NA	4	3
Autosomal recessive	NA	6	6
X-linked	NA	0	0
Unknown	NA	3	4
Eyes	34	20	22
Age, y	48.5 ± 23.7	49.6 ± 22.8	47.4 ± 13.2
Range	22-85 years	18-87 years	26-67 years
LogMAR	-0.04 ± 0.09	0.11 ± 0.16	0.19 ± 0.21
Kinetic visual field			
V4e (horizontal width in degrees)	NA	88.5 ± 55.8	75.23 ± 55.8
Severity group			
Mild	NA	10 (50%)	10 (45%)
Moderate	NA	7 (33%)	7 (32%)
Severe	NA	3 (15%)	5 (23%)

Values are given as n or n (%) or as mean ± standard deviation.
CME = cystoid macular edema; LogMAR = logarithm of the minimum angle of resolution; NA = not applicable; RP = retinitis pigmentosa.

association between history of CME and VF severity in RP patients. Spearman rank correlation coefficient and scatterplots were used, after averaging measurements from both eyes, to assess the correlation between VD in retinal plexuses and outer retinal thickness in the perifoveal region.

RESULTS

• **SUBJECT DEMOGRAPHICS AND CLINICAL DATA:** Forty-four eyes from 26 RP patients (mean age ± SD, 48.4 ± 18.2 years; range, 18-85 years) and 34 age-matched eyes from 26 normal controls (mean age ± SD, 48.5 ± 23.7 years; range, 22-85 years) were included. All patients had clinical manifestations of RP and 14 patients were genetically confirmed. Detected genetic mutations are described in the Supplemental Table (Supplemental Material available at AJO.com). RP patients were subdivided into 2 groups based on the presence of cystoid macular edema (CME) (20 eyes from 13 subjects had no history of CME; 22 eyes from 13 subjects had CME). CME was extracted from clinical records and based on the clinical assessment of OCT appearance. There was no significant difference in age between groups (ANOVA, $P = .94$). Visual acuity was statistically different between the groups (ANOVA, $P < .001$). Healthy subjects had significantly better visual acuity than both groups of RP patients (Games-Howell post hoc test, $P < .002$). Patients in the CME group tended to have a slightly worse central vision than patients with no history of CME. However, the mean visual acuity was statistically equivalent in RP patients with and without CME (Games-Howell post hoc test, $P = .38$). Similarly, patients in both groups did not show significant differences in the horizontal width of their central visual field (generalized estimating equation, $P = .53$). Additionally, no significant association was observed between the presence of CME and VF severity in patients (likelihood ratio χ^2 test, $P = .82$). Characteristics of the included participants and eyes are presented in Table 1.

• **STRUCTURAL OPTICAL COHERENCE TOMOGRAPHY:** Cross-sectional OCT images and thickness maps in RP patients showed outer retinal loss with relative sparing in the fovea (Figure 2). Loss of photoreceptors including the ellipsoid zone (EZ) and ONL layers was observed in all patients with varying degree of disease severity. Tissue loss was more pronounced in the periphery. The tissue loss was quantified by the significant reduction in outer retinal thickness in RP patients (with and without CME) compared to controls in the parafoveal and perifoveal regions (Table 2). The outer retinal degeneration was more severe in CME patients compared to the patients without CME (-48.3% change, $P < .001$).

In contrast, a significant increase in inner retinal thickness was observed in RP patients compared to healthy subjects in all sectors (Table 2). Patients with CME also showed cystic spaces within inner retinal layers. Cysts were located mainly within the parafovea, and rarely in the more peripheral perifovea (Figure 2). These cystic changes were accompanied by a significant 18.5% increase in inner retinal thickness in the parafoveal region of CME eyes compared to RP patients without CME ($P < 0.001$). No significant difference was observed in the perifoveal inner retinal thickness of RP patients between the CME and no CME groups ($P = .28$).

• **OPTICAL COHERENCE TOMOGRAPHY ANGIOGRAPHY:** Qualitative assessment of en face OCT angiograms of RP patients showed vascular attenuation in retinal circulation compared to normal controls (Figure 2). The vascular loss was more noticeable in the peripheral portions of deeper plexuses.

The inner retinal slab comprises a combination of the SVC, ICP, and DCP. Quantitatively, significant reduction in VD in the perifoveal region of the inner retinal slab was

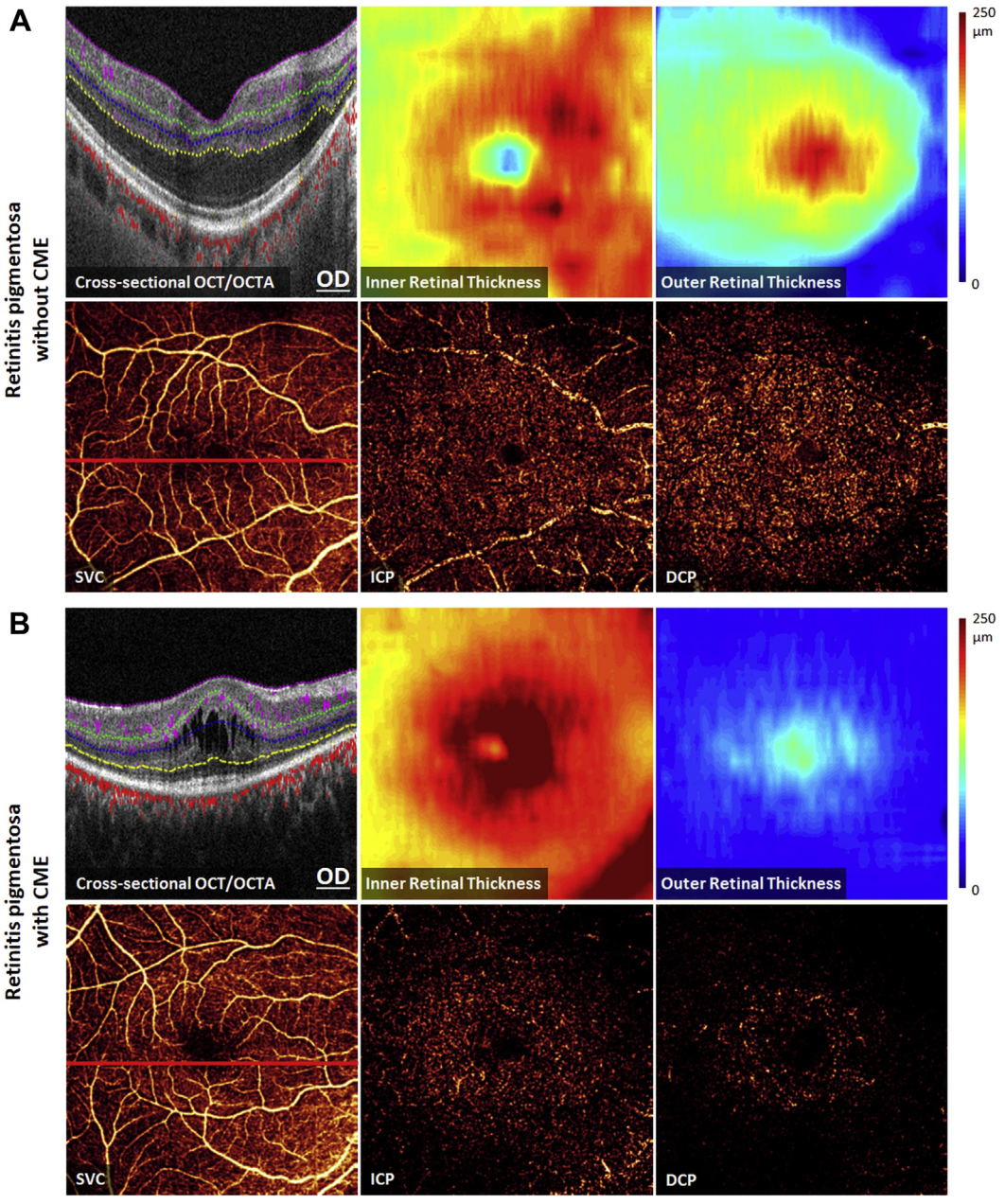

FIGURE 2. Optical coherence tomography (OCT) and OCT angiography (OCTA) 6 × 6 mm^2 macular scans from the right eyes of retinitis pigmentosa patients without cystoid macular edema (CME) (A), and with CME (B). Structural OCTA and thickness maps show outer retinal thinning that is most severe in the perifoveal region. There is relative sparing of the superficial vascular complex (SVC) compared to more severe capillary loss in the intermediate capillary plexus (ICP) and the deep capillary plexus (DCP).

observed in RP patients compared to normal controls. Patients with history of CME showed more severe hypoperfusion than the no CME group (-13.7%, $P < .001$, and -8.3%, $P = .04$, respectively). In contrast, VD of the inner retinal slab in the parafovea was statistically equivalent between groups (Table 2).

However, significant findings emerge when retinal plexuses are investigated individually, especially in the perifoveal region (Table 2). The perifoveal region of the DCP showed the greatest extent of vascular change in RP groups compared to healthy controls, with 49.4% loss in CME eyes ($P < .001$) and 31.4% loss in RP patients without CME ($P < .001$). In addition, vessel density of the perifoveal ICP in the CME group showed a significant decrease compared to the control ($P < .001$). On the contrary, no significant difference was observed for the VD of the perifoveal SVC in RP eyes. In the parafovea, although there was no significant difference in VD in the ICP or DCP compared to controls, a small but significant increase in VD was detected in the SVC of RP eyes with CME (8.3%, $P = .005$).

TABLE 2. Vessel Density and Thickness Measurements in Control and Retinitis Pigmentosa Groups

				Control vs No CME		Control vs CME		No CME vs CME	
	Control	RP Without CME	RP With CME	% Change	*P* Value	% Change	*P* Value	% Change	*P* Value
Inner retina (%)									
Parafovea	80.55 ± 10.80	79.00 ± 15.90	80.74 ± 6.27	-1.9%	.44	0.2%	.93	2.2%	.53
Perifovea	77.15 ± 11.18	70.72 ± 11.37	66.58 ± 8.22	-8.3%	.04*	-13.7%	<.001*	-5.8%	.26
SVC (%)									
Parafovea	65.76 ± 7.40	68.42 ± 11.27	71.19 ± 5.42	4.0%	.48	8.3%	.005	4.1%	.34
Perifovea	65.74 ± 5.24	65.86 ± 4.7	66.07 ± 5.70	0.2%	.56	0.5%	.83	0.3%	.95
ICP (%)									
Parafovea	50.46 ± 5.65	47.65 ± 9.71	47.89 ± 6.25	-5.6%	.24	-5.1%	.11	-0.5%	.83
Perifovea	46.73 ± 7.10	43.74 ± 7.28	39.87 ± 4.73	-6.4%	.14	-14.7%	<.001*	-8.8%	.10
DCP (%)									
Parafovea	21.16 ± 4.04	21.12 ± 6.84	20.79 ± 6.76	-0.2%	.76	-1.8%	.81	1.6%	.80
Perifovea	25.87 ± 5.71	17.74 ± 7.72	13.10 ± 4.90	-31.4%	<.001*	-49.4%	<.001*	-26.2%	.09
Outer retinal thickness (μm)									
Parafovea	147.91 ± 10.53	119.15 ± 32.18	79.56 ± 26.66	-19.4%	<.001*	-46.2%	<.001*	-33.2%	.003*
Perifovea	133.08 ± 8.05	84.73 ± 28.21	43.79 ± 13.95	-36.3%	<.001*	-67.1%	<.001*	-48.3%	<.001*
Inner retinal thickness (μm)									
Parafovea	179.36 ± 10.86	192.24 ± 22.10	227.87 ± 33.39	7.2%	<.08	27.0%	<.001*	18.5%	<.001*
Perifovea	150.59 ± 10.44	175.58 ± 22.59	188.30 ± 27.47	16.6%	<.001*	25.0%	<.001*	7.2%	.28

P values were based on generalized estimating equation (accounting for the within-subject correlation between the 2 eyes), and adjusted for multiple comparisons using Holm-Bonferroni method.

P values <0.05 were marked by an asterisk (*), indicating signifacnt differences.

CME = cystoid macular edema; DCP = deep capillary plexus; ICP = intermediate capillary plexus; RP = retinitis pigmentosa; SVC = superficial vascular complex.

• **CORRELATION BETWEEN PERIFOVEAL VESSEL DENSITY AND OUTER RETINAL THICKNESS:** The perifoveal outer retinal thickness was plotted against the perifoveal VD in the SVC, ICP, and DCP. Patients with and without CME were plotted separately. A very strong positive correlation was observed between perifoveal outer retinal thickness and VD in the DCP of patients without CME (Spearman's rho = 0.96, $P < .001$) (Figure 3). Additionally, VD of the ICP correlated moderately (rho = 0.52) with outer retinal thickness, yet it was marginally insignificant ($P = .07$). No correlation between VD and retinal thickness was detected in the SVC, as well as in patients with CME (rho < 0.36, $P > .22$).

DISCUSSION

RETINAL VASCULAR ATTENUATION IS A HALLMARK OF RP, especially in advanced disease.[2,49] In the present study, we used PR-OCTA to characterize vascular loss in the 3 distinct macular plexuses and 2 regions in RP patients. The greatest changes were observed in the perifoveal regions of the deeper retinal plexuses, the DCP and ICP. In contrast, no vascular loss was detected in the SVC. We also observed decreased outer retinal thickness and increased inner retinal thickness in RP patients compared to the age-matched healthy controls. Positive correlation was found between vessel density in the perifoveal DCP and ICP and outer retinal thickness in RP patients without history of CME. However, interestingly this correlation was lost in RP patients with CME. There was not a correlation of retinal thickness and SVC density of either group.

In RP, retinal pathology often begins in the midperiphery, with central vision remaining relatively preserved until later stages of the disease.[2] Histopathologic studies reveal that shortening of photoreceptors' outer segments is the earliest change in RP, with subsequent death and decreased number of rods and cones.[50] These findings agree with our structural OCT results of EZ defects and decreased outer retinal thickness, especially in the more peripheral regions.[51–55] Patients with CME showed more outer retinal degeneration than RP patients without history of CME, which could indicate that presence of CME might be associated with more advanced forms of RP. However, the history of CME did not correlate with the severity of the disease as measured by visual fields. Alternatively, macular atrophy, which can occur in some forms of RP, may be a risk factor for CME. We observed an increase of inner retinal thickness in RP patients with and without CME. Aside from the increased thickness resulting from inner retinal cysts in the parafovea, thickening has also been hypothesized to occur because of remodeling by retinal neurons and glial proliferation.[51] Several retinal modifications, including cellular hypertrophy, hyperplasia,

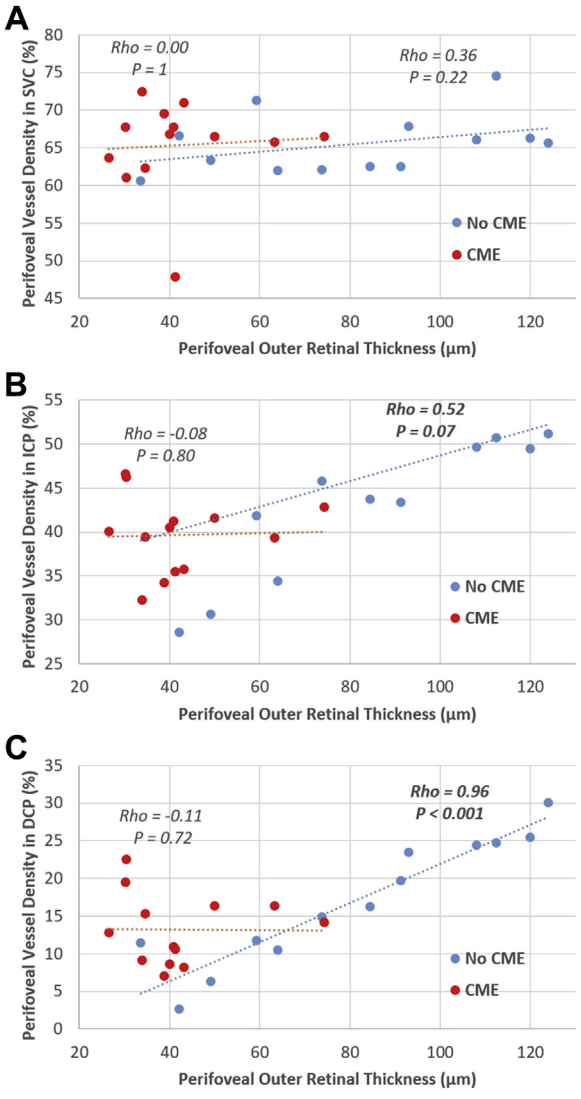

FIGURE 3. The relationship between perifoveal outer retinal thickness and perifoveal vessel density in the superficial vascular complex (SVC, A), intermediate capillary plexus (ICP, B), and deep capillary plexus (DCP, C). Scatterplots were generated from retinitis pigmentosa (RP) patients with history of cystoid macular edema (CME, red) and without history of CME (No CME, blue). Spearman's rho and *P* values of the slope are based on Spearman rank correlation test. No significant correlation was observed between the SVC and the outer retinal thickness. Moderate/strong correlations were found between the ICP/DCP vessel densities and outer retinal thickness in RP eyes without CME but not in patients with CME.

neuronal migration, and network rewiring, have been previously described within the inner retina of RP patients.[52] Several studies have previously reported similar results of EZ disruption and thinning of ONL,[53–55] as well as thickening of inner retinal layers.[56,57]

Microvascular attenuation was observed on OCT angiograms of RP patients at the perifoveal regions of the DCP and ICP. Although it has been previously suggested that the vascular component of RP might play a primary role in disease pathophysiology,[49,58] it is more commonly accepted that the decrease in retinal perfusion is secondary to photoreceptor degeneration.[57,59,60] The findings of the recent hyperoxia experiments suggest that deeper retinal plexuses, especially the DCP, contribute to the nourishment of outer retinal layers, along with choroidal circulation.[39] Thus, we expected that outer retinal degeneration will cause a decrease in metabolic demand and, consequently, secondary vascular remodeling and attenuation. This hypothesis was further supported by the strong correlation between perifoveal changes in the VD in the DCP and ICP, and the perifoveal outer retinal thickness in RP patients with no history of CME. Based on the same concepts, we can explain the relative preservation of vessel density in the parafoveal regions. Most RP patients have preservation of foveal cones and retain good central visual function until late stages of the disease. Thus, one would not expect a significant drop in the metabolic demand or a significant change in vascular density.

Furthermore, it has been suggested that the photoreceptor loss and decreased outer retinal thickness can lead to increased oxygen diffusion from the choroid into the more superficial retina,[25,61,62] resulting in autoregulatory vasoconstriction and decrease in blood flow,[25,57,63] especially in the DCP and ICP, which are anatomically closer to the choroidal layers. On the other hand, the SVC was spared and no microvascular defects were observed. The SVC is expected to be responsible for blood supply to inner retinal layers, but not the outer retinal layers. Thus, pathophysiologically, we would predict the SVC to be spared to cover the metabolic needs of the preserved inner retina and their remodeling processes occurring in RP patients. Moreover, the SVC is located away from the choroid, compared to the deeper plexuses. Therefore, the superficial plexus would not be affected by the increased oxygen supply from the choroidal circulation.[39]

We did not find correlation between outer retinal thickness and VD in patients with history of CME, which might argue for different pathophysiological pathways in those retinas. Generally, the incidence of CME was associated with significant decrease in outer retinal thickness. Furthermore, we observed an increase in vessel density for eyes with CME at the same given thickness as compared to RP eyes without CME (Figure 3). We do not know whether the loss of photoreceptors or an inflammatory process associated with CME induced proliferation of blood vessels and formation of cysts, or if the presence of CME causes an increase in vasculature as an attempt to drain macular edema. However, the cross-sectional design of this study cannot establish causality. Another possible explanation is that CME predominantly develops within the INL,[64] leading to dislocation and/or disorganization of capillaries in the ICP and DCP.

Reduced perfusion in RP was previously investigated using FA,[16] color Doppler ultrasonography,[65] bidirectional

laser Doppler velocimetry,[25] confocal laser Doppler flowmetry,[66] laser speckle flowgraphy,[26] and functional magnetic resonance imaging.[18,67] Several recent studies used OCTA to characterize the microvascular changes. Generally, they reported decreased vessel density in RP patients compared to controls, which agrees with the findings of our study. However, these studies used the commercial software, which uses a 2-layer scheme to divide retinal circulation into superficial and deep plexuses, leading to faulty placement of most of the ICP with the superficial plexus slab. Thus, most previous studies reported decreased vessel density in the deep plexus, as well as the superficial plexus, which is actually caused by the defects in the intermediate plexus, not the superficial. In addition, previous investigations observed decreased perfusion in the parafoveal region of RP patients, in which we found no statistically significant changes compared to age-matched healthy participants. These differences might be caused by variations in image processing methods. The variation in signal strength index and the presence of projection artifacts can substantially alter OCTA measurements. Hence, projection-resolved and reflectance compensation algorithms were applied in our method to significantly eliminate the impacts of these artifacts. In contrast, commercial software does not employ such strategies, which can potentially introduce erroneous measurements and analyses.

The findings of this study not only provided potential clinical trial endpoints, but also gave insight into the pathophysiology of RP. Still, there were several limitations that might need to be addressed in future work. Cross-sectional design, modest number of participants, and lack of genetic characterization are major limitations. Longitudinal studies with larger sample size and detailed genetic information might provide more conclusive results and reveal associations between microvascular alterations and specific gene mutations. Moreover, we did not correlate the microvascular parameters with functional parameters, including visual acuity, retinal sensitivity on microperimetry, and ERG.

In conclusion, OCT and PR-OCTA were able to characterize the structural and microvascular changes at distinct macular layers in the parafoveal and perifoveal regions of RP patients. They showed thinner outer retina and thicker inner retina, as well as decreased vessel density in the perifovea of DCP and ICP, with relative sparing of the SVC. Vessel density in the perifovea of DCP and ICP correlated strongly with outer retinal thickness in RP patients without history of CME. However, these correlations break down with the development of CME, with an observed increase in vessel density. Our findings suggest that OCT and OCTA parameters might be able to provide better understanding of the pathophysiology of the disease, as well as monitoring disease progression and the response to experimental treatments.

FUNDING/SUPPORT: THIS WORK WAS SUPPORTED BY GRANTS R01 EY027833, R01 EY024544, P30 EY010572, AND K08 EY026650 FROM the National Institutes of Health (Bethesda, Maryland, USA), and C-CL-0711-0534-OHSU01 and career development grant CD-NMT-0714-0648 from Foundation Fighting Blindness, and an unrestricted departmental funding grant and William & Mary Greve Special Scholar Award from Research to Prevent Blindness (New York, New York, USA). Financial Disclosures: Oregon Health & Science University (OHSU), David Huang, and Yali Jia have a significant financial interest in Optovue, Inc, a company that may have a commercial interest in the results of this research and technology. Richard G. Weleber and Mark E. Pennesi serve on advisory boards for Foundation Fighting Blindness These potential conflicts of interest have been reviewed and managed by OHSU. The following authors have no financial disclosures: Ahmed M. Hagag, Jie Wang, Kevin Lu, Gareth Harman, and Paul Yang. All authors attest that they meet the current ICMJE criteria for authorship.

REFERENCES

1. RetNet. Available at: http://www.sph.uth.tmc.edu/RetNet/. Accessed August, 2018.
2. Hartong DT, Berson EL, Dryja TP. Retinitis pigmentosa. *Lancet* 2006;368(9549):1795–1809.
3. Berson EL, Sandberg MA, Rosner B, Birch DG, Hanson AH. Natural course of retinitis pigmentosa over a three-year interval. *Am J Ophthalmol* 1985;99(3):240–251.
4. Bunker CH, Berson EL, Bromley WC, Hayes RP, Roderick TH. Prevalence of retinitis pigmentosa in Maine. *Am J Ophthalmol* 1984;97(3):357–365.
5. Jacobson SG, Cideciyan AV. Treatment possibilities for retinitis pigmentosa. *N Engl J Med* 2010;363(17):1669–1671.
6. Sahni JN, Angi M, Irigoyen C, Semeraro F, Romano MR, Parmeggiani F. Therapeutic challenges to retinitis pigmentosa: from neuroprotection to gene therapy. *Curr Genomics* 2011;12(4):276–284.
7. Holopigian K, Greenstein V, Seiple W, Carr RE. Rates of change differ among measures of visual function in patients with retinitis pigmentosa. *Ophthalmology* 1996;103(3):398–405.
8. Sandberg MA, Weigel-DiFranco C, Rosner B, Berson EL. The relationship between visual field size and electroretinogram amplitude in retinitis pigmentosa. *Invest Ophthalmol Vis Sci* 1996;37(8):1693–1698.
9. Berson EL, Rosner B, Sandberg MA, et al. A randomized trial of vitamin A and vitamin E supplementation for retinitis pigmentosa. *Arch Ophthalmol* 1993;111(6):761–772.
10. Grover S, Fishman GA, Birch DG, Locke KG, Rosner B. Variability of full-field electroretinogram responses in subjects without diffuse photoreceptor cell disease. *Ophthalmology* 2003;110(6):1159–1163.
11. Bittner AK, Iftikhar MH, Dagnelie G. Test-retest, within-visit variability of Goldmann visual fields in retinitis pigmentosa. *Invest Ophthalmol Vis Sci* 2011;52(11):8042–8046.

12. Huang D, Swanson EA, Lin CP, et al. Optical coherence tomography. *Science* 1991;254(5035):1178–1181.
13. Apushkin MA, Fishman GA, Alexander KR, Shahidi M. Retinal thickness and visual thresholds measured in patients with retinitis pigmentosa. *Retina* 2007;27(3):349–357.
14. Sandberg MA, Brockhurst RJ, Gaudio AR, Berson EL. The association between visual acuity and central retinal thickness in retinitis pigmentosa. *Invest Ophthalmol Vis Sci* 2005;46(9):3349–3354.
15. Garcia-Martin E, Pinilla I, Sancho E, et al. Optical coherence tomography in retinitis pigmentosa: reproducibility and capacity to detect macular and retinal nerve fiber layer thickness alterations. *Retina* 2012;32(8):1581–1591.
16. Krill AE, Archer D, Newell FW. Fluorescein angiography in retinitis pigmentosa. *Am J Ophthalmol* 1970;69(5):826–835.
17. Langham ME, Kramer T. Decreased choroidal blood flow associated with retinitis pigmentosa. *Eye (Lond)* 1990;4(Pt 2):374–381.
18. Zhang Y, Harrison JM, Nateras OS, Chalfin S, Duong TQ. Decreased retinal-choroidal blood flow in retinitis pigmentosa as measured by MRI. *Doc Ophthalmol* 2013;126(3):187–197.
19. Spaide RF, Klancnik JM Jr, Cooney MJ. Retinal vascular layers imaged by fluorescein angiography and optical coherence tomography angiography. *JAMA Ophthalmol* 2015;133(1):45–50.
20. Yannuzzi LA, Rohrer KT, Tindel LJ, et al. Fluorescein angiography complication survey. *Ophthalmology* 1986;93(5):611–617.
21. Jia Y, Tan O, Tokayer J, et al. Split-spectrum amplitude-decorrelation angiography with optical coherence tomography. *Opt Express* 2012;20(4):4710–4725.
22. Hagag AM, Gao SS, Jia Y, Huang D. Optical coherence tomography angiography: Technical principles and clinical applications in ophthalmology. *Taiwan J Ophthalmol* 2017;7(3):115–129.
23. Jia Y, Bailey ST, Hwang TS, et al. Quantitative optical coherence tomography angiography of vascular abnormalities in the living human eye. *Proc Natl Acad Sci U S A* 2015;112(18):E2395–E2402.
24. Gao SS, Jia Y, Zhang M, et al. Optical coherence tomography angiography. *Invest Ophthalmol Vis Sci* 2016;57(9):OCT27–OCT36.
25. Grunwald JE, Maguire AM, Dupont J. Retinal hemodynamics in retinitis pigmentosa. *Am J Ophthalmol* 1996;122(4):502–508.
26. Murakami Y, Ikeda Y, Akiyama M, et al. Correlation between macular blood flow and central visual sensitivity in retinitis pigmentosa. *Acta Ophthalmol* 2015;93(8):e644–e648.
27. Toto L, Borrelli E, Mastropasqua R, et al. Macular features in retinitis pigmentosa: correlations among ganglion cell complex thickness, capillary density, and macular function. *Invest Ophthalmol Vis Sci* 2016;57(14):6360–6366.
28. Spaide RF, Fujimoto JG, Waheed NK. Image artifacts in optical coherence tomography angiography. *Retina* 2015;35(11):2163–2180.
29. Provis JM. Development of the primate retinal vasculature. *Prog Retin Eye Res* 2001;20(6):799–821.
30. Battaglia Parodi M, Cicinelli MV, Rabiolo A, et al. Vessel density analysis in patients with retinitis pigmentosa by means of optical coherence tomography angiography. *Br J Ophthalmol* 2017;101(4):428–432.
31. Koyanagi Y, Murakami Y, Funatsu J, et al. Optical coherence tomography angiography of the macular microvasculature changes in retinitis pigmentosa. *Acta Ophthalmol* 2018;96(1):e59–e67.
32. Takagi S, Hirami Y, Takahashi M, et al. Optical coherence tomography angiography in patients with retinitis pigmentosa who have normal visual acuity. *Acta Ophthalmol* 2018;96(5):e636–e642.
33. Zhang M, Hwang TS, Campbell JP, et al. Projection-resolved optical coherence tomographic angiography. *Biomed Opt Express* 2016;7(3):816–828.
34. Wang J, Zhang M, Hwang TS, et al. Reflectance-based projection-resolved optical coherence tomography angiography [Invited]. *Biomed Opt Express* 2017;8(3):1536–1548.
35. Campbell JP, Zhang M, Hwang TS, et al. Detailed vascular anatomy of the human retina by projection-resolved optical coherence tomography angiography. *Sci Rep* 2017;7:42201.
36. Patel RC, Wang J, Hwang TS, et al. Plexus-specific detection of retinal vascular pathologic conditions with projection-resolved OCT angiography. *Ophthalmol Retina* 2018;2(8):816–826.
37. Hwang TS, Zhang M, Bhavsar K, et al. Visualization of 3 distinct retinal plexuses by projection-resolved optical coherence tomography angiography in diabetic retinopathy. *JAMA Ophthalmol* 2016;134(12):1411–1419.
38. Takusagawa HL, Liu L, Ma KN, et al. Projection-resolved optical coherence tomography angiography of macular retinal circulation in glaucoma. *Ophthalmology* 2017;124(11):1589–1599.
39. Hagag AM, Pechauer AD, Liu L, et al. OCT angiography changes in the 3 parafoveal retinal plexuses in response to hyperoxia. *Ophthalmol Retina* 2018;2(4):329–336.
40. Hwang TS, Hagag AM, Wang J, et al. Automated quantification of nonperfusion areas in 3 vascular plexuses with optical coherence tomography angiography in eyes of patients with diabetes. *JAMA Ophthalmol* 2018;136(8):929–936.
41. Xue J, Camino A, Bailey ST, Liu X, Li D, Jia Y. Automatic quantification of choroidal neovascularization lesion area on OCT angiography based on density cell-like P systems with active membranes. *Biomed Opt Express* 2018;9(7):3208–3219.
42. Lu Y, Simonett JM, Wang J, et al. Evaluation of automatically quantified foveal avascular zone metrics for diagnosis of diabetic retinopathy using optical coherence tomography angiography. *Invest Ophthalmol Vis Sci* 2018;59(6):2212–2221.
43. McClintic SM, Gao S, Wang J, et al. Quantitative evaluation of choroidal neovascularization under pro re nata anti-vascular endothelial growth factor therapy with OCT angiography. *Ophthalmol Retina* 2018;2(9):931–941.
44. Zhang M, Hwang TS, Dongye C, Wilson DJ, Huang D, Jia Y. Automated quantification of nonperfusion in three retinal plexuses using projection-resolved optical coherence tomography angiography in diabetic retinopathy. *Invest Ophthalmol Vis Sci* 2016;57(13):5101–5106.
45. Skalet AH, Liu L, Binder C, et al. Quantitative OCT angiography evaluation of peripapillary retinal circulation after plaque brachytherapy. *Ophthalmol Retina* 2018;2(3):244–250.
46. Zhang M, Wang J, Pechauer AD, et al. Advanced image processing for optical coherence tomographic angiography of macular diseases. *Biomed Opt Express* 2015;6(12):4661–4675.

47. Gao SS, Jia Y, Liu L, et al. Compensation for reflectance variation in vessel density quantification by optical coherence tomography angiography. *Invest Ophthalmol Vis Sci* 2016; 57(10):4485–4492.
48. Jia Y, Simonett JM, Wang J, et al. Wide-field OCT angiography investigation of the relationship between radial peripapillary capillary plexus density and nerve fiber layer thickness. *Invest Ophthalmol Vis Sci* 2017;58(12):5188–5194.
49. Cellini M, Strobbe E, Gizzi C, Campos EC. ET-1 plasma levels and ocular blood flow in retinitis pigmentosa. *Can J Physiol Pharmacol* 2010;88(6):630–635.
50. Milam AH, Li ZY, Fariss RN. Histopathology of the human retina in retinitis pigmentosa. *Prog Retin Eye Res* 1998; 17(2):175–205.
51. Jones BW, Marc RE. Retinal remodeling during retinal degeneration. *Exp Eye Res* 2005;81(2):123–137.
52. Jones BW, Pfeiffer RL, Ferrell WD, Watt CB, Marmor M, Marc RE. Retinal remodeling in human retinitis pigmentosa. *Exp Eye Res* 2016;150:149–165.
53. Liu G, Liu X, Li H, Du Q, Wang F. Optical Coherence Tomographic Analysis of Retina in Retinitis Pigmentosa Patients. *Ophthalmic Res* 2016;56(3):111–122.
54. Lim JI, Tan O, Fawzi AA, Hopkins JJ, Gil-Flamer JH, Huang D. A pilot study of Fourier-domain optical coherence tomography of retinal dystrophy patients. *Am J Ophthalmol* 2008;146(3):417–426.
55. Lima LH, Cella W, Greenstein VC, et al. Structural assessment of hyperautofluorescent ring in patients with retinitis pigmentosa. *Retina* 2009;29(7):1025–1031.
56. Aleman TS, Cideciyan AV, Sumaroka A, et al. Inner retinal abnormalities in X-linked retinitis pigmentosa with RPGR mutations. *Invest Ophthalmol Vis Sci* 2007;48(10):4759–4765.
57. Verbakel SK, van Huet RAC, Boon CJF, et al. Non-syndromic retinitis pigmentosa. *Prog Retin Eye Res* 2018;66: 157–186.
58. Konieczka K, Flammer AJ, Todorova M, Meyer P, Flammer J. Retinitis pigmentosa and ocular blood flow. *EPMA J* 2012; 3(1):17.
59. Stone JL, Barlow WE, Humayun MS, de Juan E Jr, Milam AH. Morphometric analysis of macular photoreceptors and ganglion cells in retinas with retinitis pigmentosa. *Arch Ophthalmol* 1992;110(11):1634–1639.
60. Rangaswamy NV, Patel HM, Locke KG, Hood DC, Birch DG. A comparison of visual field sensitivity to photoreceptor thickness in retinitis pigmentosa. *Invest Ophthalmol Vis Sci* 2010;51(8):4213–4219.
61. Padnick-Silver L, Kang Derwent JJ, Giuliano E, Narfstrom K, Linsenmeier RA. Retinal oxygenation and oxygen metabolism in Abyssinian cats with a hereditary retinal degeneration. *Invest Ophthalmol Vis Sci* 2006;47(8):3683–3689.
62. Penn JS, Li S, Naash MI. Ambient hypoxia reverses retinal vascular attenuation in a transgenic mouse model of autosomal dominant retinitis pigmentosa. *Invest Ophthalmol Vis Sci* 2000;41(12):4007–4013.
63. Yu DY, Cringle SJ. Retinal degeneration and local oxygen metabolism. *Exp Eye Res* 2005;80(6):745–751.
64. Makiyama Y, Oishi A, Otani A, et al. Prevalence and spatial distribution of cystoid spaces in retinitis pigmentosa: investigation with spectral domain optical coherence tomography. *Retina* 2014;34(5):981–988.
65. Cellini M, Lodi R, Possati GL, Sbrocca M, Pelle D, Giubilei N. [Color Doppler ultrasonography in retinitis pigmentosa. Preliminary study]. *J Fr Ophtalmol* 1997;20(9): 659–663.
66. Falsini B, Anselmi GM, Marangoni D, et al. Subfoveal choroidal blood flow and central retinal function in retinitis pigmentosa. *Invest Ophthalmol Vis Sci* 2011;52(2):1064–1069.
67. Muir ER, De La Garza B, Duong TQ. Blood flow and anatomical MRI in a mouse model of retinitis pigmentosa. *Magn Reson Med* 2013;69(1):221–228.